

SUPER/ZERO SCATTERING CHARACTERISTICS OF CIRCULAR SRR ARRAYS

Yuan Zhang^{1, 2}, Erik Forsberg¹, and Sailing He^{1, 2, 3, *}

¹Centre for Optical and Electromagnetic Research, Zhejiang Provincial Key Laboratory for Sensing Technologies, JORCEP [Sino-Sweden Joint Research Center of Photonics], Zhejiang University, Hangzhou, China

²ZJU-SCNU Joint Research Center of Photonics, South China Normal University, Guangzhou 510006, China

³ Department of Electromagnetic Engineering, Royal Institute of Technology, Stockholm 100 44, Sweden

Abstract—The ability to control the scattering property of an object is important in many applications. In this paper, we propose and study the scattering characteristics of a circular array of split-ring resonators (SRRs). By calculating the scattered energy spectrum, we show that the proposed structure has a localized surface plasmon resonance like behavior, which makes it useful as a super scatterer. Furthermore, in a special case, the proposed structure exhibits transparency to the illuminated waves, i.e., it does not scatter any energy at all and thus acts as a zero electromagnetic scattering object.

1. INTRODUCTION

The past ten years have seen a significant development of the field of metamaterials [1–6]. The strong interest is motivated by the possibility to tailor the electromagnetic response that a periodic structure of metamaterials allows, which promises to have a significant impact in physics, optics and material science. Effective permittivities and permeabilities of metamaterials designed to range from negative to positive values have many important applications such as invisible cloaks [7–10], superlenses [11–13], microwave horn antennas [14] as well as other electromagnetic devices [15, 16].

Received 6 February 2013, Accepted 28 February 2013, Scheduled 4 March 2013

* Corresponding author: Sailing He (sailing@jorcep.org).

The scattering characteristics of an object are of big importance in many applications and hence the ability to be able to manipulate it is of strong interest. In military applications the desire is often to achieve a scattering cross section as small as possible, e.g., to hide an aircraft from enemy radar, which is the original motivation for metamaterial cloaking [7–10]. In contrast, other applications benefit from an increased scattering cross section as in the case of certain passive RFID tags or metallic nanoparticles in surface-enhanced Raman scattering (SERS) applications [17].

In parallel to the development of metamaterials, surface plasmons (SPs) at metal-dielectric surfaces have received similarly strong attention these past 10 years [18–21]. This is again due to interesting potential applications of either surface plasmon polaritons (SPPs) propagating on extended surfaces or in waveguides, or localized surface plasmons (LSPs) on closed surfaces [19]. LSPs can, e.g., allow noble metal particles of sub-wavelength volume scale to scatter a much larger amount of energy than a dielectric object of the same size [22]. However, in the microwave band a metal will act as a perfectly electrically conductor (PEC) preventing plasmonic effects to be achieved. It is however still possible to extend plasmonic effects to the microwave and terahertz bands by using spoofed metal surfaces [23–26]. For a spoof SPP wave, the analogous surface plasmon frequency corresponds to the lowest mode frequency of the individual metal cavity [23].

In the same manner as a SPP wave on a metal/dielectric interface, a spoofed SPP is polarization sensitive and can only support a surface wave that has an electric field component along its propagation direction. This is linked to the cavity mode property of the metal cavity, which can be treated as an electric resonator. Would it however be possible to achieve a similar behavior for another polarization? One possibility to achieve this is to modify a surface using magnetic rather than electric resonators. In this paper we propose a structure based on metamaterial elements having controllable scattering characteristics. Using split-ring resonators arranged in a circular array, we show that the structure can demonstrate both super and zero scattering properties.

2. THE DISPERSION RELATION OF SRR ARRAYS

In our design we choose to use a typical magnetic metamaterial unit cell, a split-ring resonator (SRR), to replace the metal cavity, and arrange the SRRs in a periodic pattern (see Figure 1(c)). It is reasonable to expect such a structure will have a SPP effect analogous to that found in spoofed metals but for a different polarization.

The SRR element is composed of two square PEC frames, with the geometry parameters of the SRR (as indicated in Figure 1(a)) being: $d = 3$ mm, $c = 2.4$ mm, $g = 0.2$ mm. The size of the unit cell is $a = 3.2$ mm and $b = 4$ mm. These two concentric PEC frames are embedded in a dielectric material with a refractive index $n = 5$ and the strips' width and thickness are 0.2 mm and 0.1 mm, respectively. The geometry of the SRR unit cell remains the same throughout this paper.

Dispersion relation curves are always used to analysis the characteristic of surface wave on metal [19] or spoofed metal [24, 25] surface. Firstly we calculate the dispersion relation of a planar array of SRRs arranged as in Figure 1(c). In the calculation, the unit cell is sandwiched by PEC boundaries normal to z axis, and periodic boundary condition normal to y axis. The PMC boundaries normal to x axis are set far enough from the structure to avoid affecting field pattern on the SRR element. Since the dispersion relation is very much related to the SRR resonance, which will be affected evidently by the refractive index of the dielectric environment (while in Section 3 we wish to calculate the electromagnetic scattering properties of a circular array of 8 SRR elements as shown in Figure 2 below), we make the profile of the upper cladding of each unit cell in Figure 1(c) arched as approximately 1/8 cylinder surface (see the shaded gray area in Figure 2(b); i.e., eight unit cell in Figure 1(c) rolled up in circle will form a whole cylinder as in Figure 2; note that z -axis is pointing into the page in Figure 1(c) while is pointing upward in Figure 2(a)). This way we wish to describe more closely the dielectric environment around the SRR elements when we study the circular SRR array in Figure 2 though the dispersion relation calculated from a planar one shown in Figure 1(c). By finding the mode frequency corresponding to every phase difference between the periodic boundaries, the dispersion relation curves are shown in Figure 1(b). It is clear that the lowest energy band (red curve) of the periodic SRR structure is similar to that of a spoofed metal surface (and thus similar to that of a SPP). The asymptote position (near 2 GHz) of the first band is close to the resonant frequency of the individual SRR element, indicating the value of the mimic SPP frequency. Here we also note that, although the thickness of the SRRs is quite thin compared to the working wavelength, the band structure of the mimic surface wave is different from that of the real surface wave on a thin metal strip. It is well known that there exist two different modes, long range surface plasmon mode and short range surface plasmon mode, caused by the symmetric and asymmetric coupling between the surface waves on both sides of the metal strip, which leads to a split branch in the dispersion relation

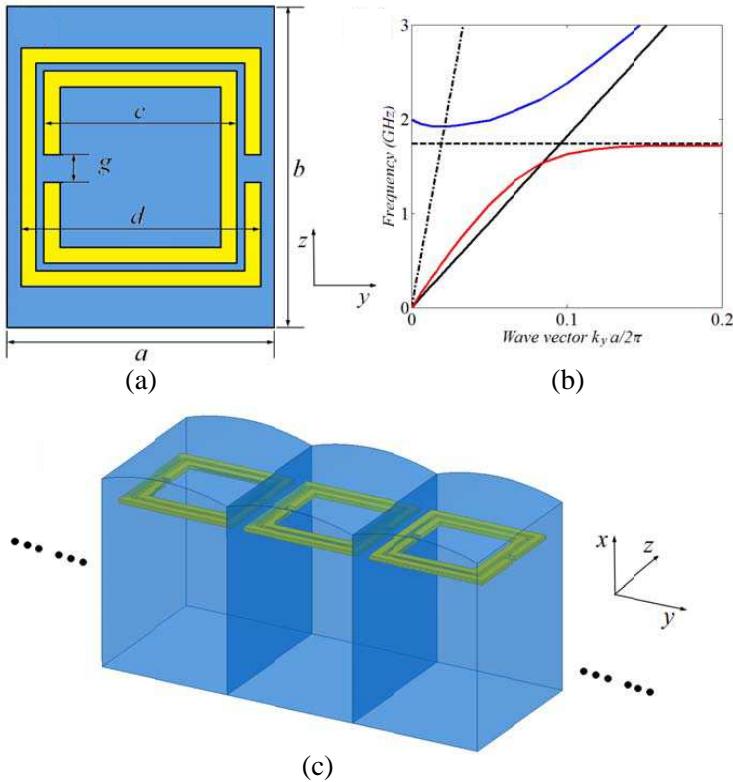


Figure 1. (a) Geometry of the SRR element (gold), embedded in a dielectric material (blue), being of finite height above the SRR element and assumed infinite below. (b) Dispersion relation of a periodic SRR element array as depicted in (c) where the dielectric material is finite height above the SRR element and assumed infinite below. Red and blue curves represent the first and second bands of the SRR periodic array. The dashed asymptote of the lowest band indicates the resonant frequency of a single SRR element. The black solid and dash-dotted lines represent the light lines of refractive indices $n = 5$ and $n = 1$, respectively.

diagram [19]. However for the mimic surface wave in Figure 1 only one branch for the surface wave mode exists, which indicates that there does not exist any coupling between the upper and lower surface waves of the SRRs. The reason for this is that the surface wave is caused by the resonance of the SRR cell. The SRR resonance stems from the overall current flow in the SRR structure, which means that the SRR

unit cell cannot be treated as having an upper and a lower surfaces and thus no separate symmetric and asymmetric modes can exist. As the upper dielectric cladding has a finite thickness (see Figure 1(c)), the dispersion curve of first band expands a somewhat to the area above the dielectric light line.

We know that the resonant frequency of a SRR can be tuned by its shape, the embedded material, and by using lumped elements; i.e., the electromagnetic response can be tailored by design to a large extent. For a spoofed SPP on the other hand, the resonance of the metal cavity (and thus the spoofed SPP frequency) can be tuned only by its simple geometry and the choice of dielectric material. Thus, the mimic surface plasmon frequency of a SRR array can be modified to a larger extent than that of a spoofed metal surface.

3. SUPER AND ZERO SCATTERING PROPERTIES OF A CIRCULAR ARRAY OF 8 SRR ELEMENTS

Based on the analogous SPP effect of the SRR array discussed in the previous section, we propose a structure that consists of a circular array of the SRR elements (Figure 2), and study its electromagnetic properties. We will demonstrate in the following below that such a structure can act as both as a super scatterer as well as a zero scatterer.

To begin with, we study a structure consisting of 8 SRR elements arranged in a circular array and embedded in a dielectric cylinder having radius $R = 5$ mm and refractive index $n = 5$. The radius of the SRR circle is $r = 4$ mm. In practical experiment, the array of SRR can be fabricated on a thin flexible substrate and curved in a circle. Then, the circular array of SRRs can be embedded in high dielectric powder which could be easy to be formed as a cylinder with high index around 5. To study its electromagnetic properties, we assume the circular SRR array to be sandwiched between two PEC boundaries normal to the z axis (i.e., the structure has infinite periods in z direction). The incident plane wave is TE polarized as shown in Figure 2(a).

Using the finite element method, we calculate the energy scattered by the circular SRR array under TE plane wave illumination in the frequency range of 1 GHz to 3 GHz. The scattering spectrum is plotted (in red) in Figure 3. For comparison, we also calculate the scattering properties of a dielectric and a PEC cylinder having the same radius ($R = 5$ mm) as the circular SRR array structure and plot the spectra in Figure 3 as well (black dashed and blue dash-dotted curves respectively). We note that the diameter of the cylinders (10 mm) is an order of magnitude smaller than the vacuum wavelength

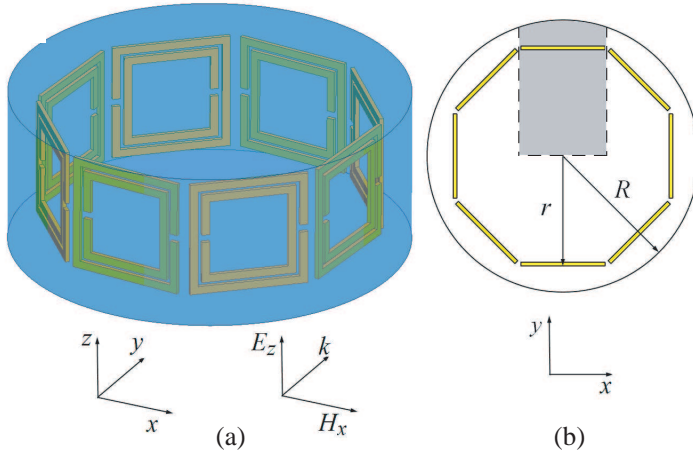


Figure 2. (a) A closed circle array consisting of SRR elements in a closed circle embedded in a dielectric cylinder base. (b) Planform of the circular SRR array. The radii of the dielectric cylinder and the SRR array are $R = 5$ mm and $r = 4$ mm. In the simulations the structure is assumed to be sandwiched between two PEC plates normal to z axis (with position of $z = -2$ mm and $z = 2$ mm). The incident plane wave is TE polarized and propagates along the y axis. The shaded gray area in (b) is used as the unit cell in the dispersion relation calculation in Section 2 (see Fig. 1(c)).

of the TE plane wave, which ranges between 300 to 100 mm at the corresponding frequency range of 1 to 3 GHz. For the PEC cylinder, the scattered energy is small and the spectrum smooth throughout the frequency range, because the diameter is much smaller than the working wavelength, and thus cannot affect the incident wave to any significant degree. The dielectric cylinder has a refractive index of $n = 5$ and therefore its real volume seen by the incident wave is comparable to the wavelength. Due to this the dielectric cylinder induces a phase change of the incident wave, which explains the slowly growing peak in its scattering spectrum, and that at most frequencies it scatters more energy than PEC cylinder.

We notice from Figure 3 that the scattering spectrum of the circular SRR array is not smooth. It includes several peaks and dips, indicating a strong electromagnetic response of the circular SRR array. To gain more insight of the interaction we plot mode field patterns for the peaks and dips of the spectrum. Note that the mode distributions are from the scattered field under plane wave illumination, and that the

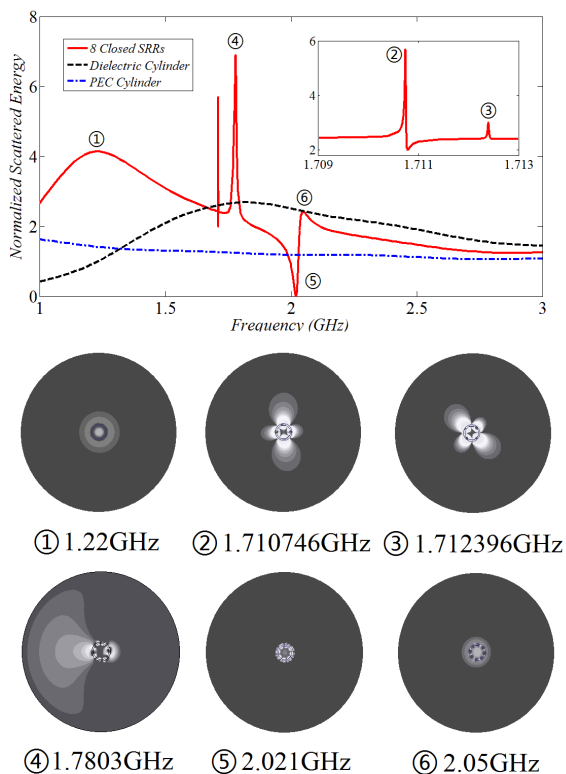


Figure 3. Red curve: The normalized total scattered energy of a TE plane wave illuminating a circular SRR array structure as depicted in Figure 2. The black dashed and blue dash-dotted curves are the spectra for a dielectric ($n = 5$) cylinder and PEC cylinder with the same radius $R = 5$ mm. The mode field patterns for the peaks and dip of the circular SRR array spectrum labeled 1–6 are plotted below the spectra.

color bar is modified specifically for each figure to ensure that the mode pattern is seen clearly. Therefore, the brightness does not represent the scattering strength. At lower frequencies (label 1 in Figure 3), we see that the spectrum has a smooth and slowly changing peak, which is very much like the scattering spectrum of the dielectric cylinder. The peak position of the circular SRR array is however red shifted as the PEC SRRs induce extra phase modulation as compared to the bare dielectric cylinder, while at same time also enhancing the scattered energy. The corresponding mode distribution is monopolar like, and

this effect remains throughout the entire spectrum as a background scattering (see, e.g., the mode distribution of the position labeled number 6, which retains a monopolar like pattern).

The sharp peaks in the spectrum numbered from 2 to 4 indicate that at certain frequencies a large amount of energy is scattered by the structure, i.e., at these frequencies the structure can work as a super scatterer. As the total diameter of the structure is much smaller than the incident wavelength (10 mm compared to about 170 mm at 1.7 GHz), it is not large enough, even though it is filled by high index material ($n = 5$), to sustain a dipolar mode as in a dielectric cylinder resonator. By inspecting the mode pattern of these modes, we find that they show a behavior analogical to that of a localized surface plasmon mode of metal particles. Mode field patterns 2 and 3 correspond to quadrupolar modes and mode field pattern 4 corresponds to a dipolar mode whose bandwidth is broader than the quadrupolar modes. Pors et al. have recently discussed similar effects of spoof SPPs [26]. Although they are both clearly localized plasmonic like modes, there are differences between what we find here and that in Ref. [26]. Generally speaking, the higher order modes occupy higher energy levels than the lower order modes (see Figure 2 in Ref. [26] and the corresponding discussion), however here we see that for our design the frequency of quadrupolar mode is lower than that of dipolar mode. This is because the structure contains only 8 SRRs, and therefore the finite period array cannot be treated as an effective homogenous plasmonic like cylinder. The finite period arrangement will have a much larger effect on the quadrupolar mode than on the dipolar mode, since the quadrupolar mode has a larger wave vector due to the structure (i.e., has a better resolution to see the unit cell). This finite unit limit will disturb the energy level of different modes. Another difference of the circular SRR array as compared to a plasmonic cylinder is that there exist two quadrupolar modes, which usually degenerate in a normal plasmonic mode. This unexpected result can most probably be explained by the asymmetric design of the SRR elements. The asymmetric feature of the SRR element is the cut position on inner and outer PEC frames, which leads to the coexistence of two quadrupolar modes with a slight energy difference.

A further important feature of the circular SRR array is that at one frequency the whole structure exhibits zero scattering. This point in the spectrum, at the frequency 2.021 GHz, is labeled mode number 5 in Figure 3. At this frequency the total scattered energy is zero, meaning that the incident plane wave passes through the circular SRR array without any disturbance, i.e., the structure cannot be seen (or detected) by the incident plane wave, an effect quite similar

to cloaking based on metamaterials. Compared to common cloaking systems, which contain dozens of metamaterial layers to “protect” the center target (see the typical cloaking in Ref. [7]), in our design, just one ultra-thin (0.1 mm) SRR surrounding layer can make a high index core invisible from an incident wave. This interesting effect happens near the resonance frequency of the SRR element. Considering the strong Fano like line shape of the scattering spectrum around 2 GHz, the cloaking effect can be explained by destructive interference between the single state (the SRR resonance) and the continuous state (the background scattering caused by the whole structure).

To further confirm the electromagnetic response behavior of the circular SRR array, we show the simulation results of the electrical field pattern in Figure 4 when the structure is illuminated by a TE plane wave. As a reference, the scattered field pattern due to scattering by a dielectric cylinder with radius $R = 5$ mm of an incident wave at frequency 1.7803 GHz is shown in Figure 4(a). As expected, some incident energy is scattered even though the cylinder has a quite small dimension compared to the incoming wavelength as the cylinder is made of a high index material. At the same frequency of the incoming wave (1.7803 GHz), Figure 4(b) shows the scattered field pattern of the circular SRR array at dipolar mode (mode number 4 in Figure 2). We

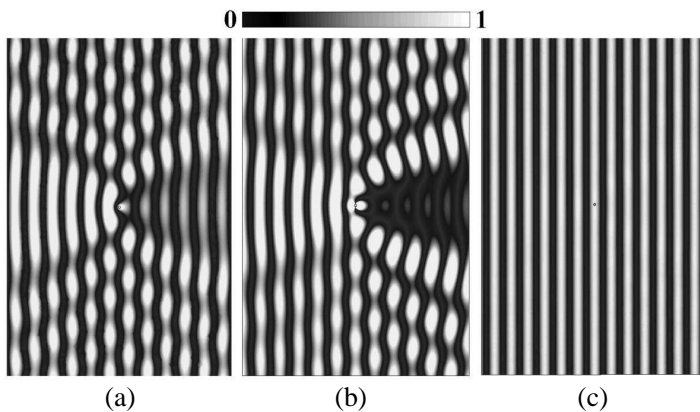


Figure 4. The electrical field distributions when an incident wave is scattered wave by (a) a dielectric cylinder with radius $R = 5$ mm at 1.7803 GHz, (b) a circular 8 element SRR array at 1.7803 GHz, corresponding to the dipolar mode number 4 in Figure 3, and (c) a circular 8 element SRR array at 2.021 GHz. The circular SRR array structure is located in the middle of each figure and is indicated by a small black circle.

can clearly see how the incident energy is blurred more heavily than is the case in Figure 4(a), i.e., the circular SRR array embedded in a dielectric structure has a stronger scattering ability than a homogenous dielectric object of the same size. We do not show the scattered field pattern of the same size PEC cylinder, as its scattering ability is weaker than the dielectric cylinder and does not yield any additional insight in this discussion. Figure 4(b) shows that a structure having a quite small size (an order of magnitude smaller than the wavelength of the illuminating wave) can scatter a large part of the energy impinging on it, i.e., it acts as a super scatterer. For mode number 5 of Figure 3, we show the scattered field pattern in Figure 4(c) to verify the zero scattering characteristics. Here we can see clearly that the incident wave (at frequency of 2.021 GHz) is not affected by the circular SRR array structure but passes smoothly through it, i.e., the circular SRR array is indeed invisible (cloaked) to the incident wave at this frequency.

4. SCATTERING SPECTRUM OF A CIRCULAR 16 ELEMENT SRR ARRAY

We now turn to study the scattering spectrum of a larger circular SRR array having a larger amount of SRR elements for which we expect a similar, *albeit* more complex, scattering spectrum as compared to that of the previous section. We study a circular 16 element SRR array embedded in a dielectric cylinder base with $R = 10$ mm. The SRR geometry is still fixed as described in Figure 1, and the radius of the circular SRR array is $r = 8$ mm.

Figure 5(a) shows the total scattered field spectrum when the circular 16-element SRR array is illuminated by a TE plane wave. Spectrum details are plotted in Figures 5(b) and 5(c). The main features of the scattering spectrum of the circular 16 element SRR array are indeed similar to that of the circular 8 element SRR array, however with a richer electromagnetic response. The increased number of SRR elements enables excitation of higher order plasmonic like modes. For a mode with fixed order, the longer perimeter of the structure means a smaller wave vector, which in turn means a larger effective wavelength, and therefore it will be less sensitive to the SRR unit cell. Mode 1 is a dipolar mode occupying the lowest energy level. Modes 6 and 7 are two quadrupolar modes that cannot degenerate due to the asymmetric detail of the SRR element. Mode 5 corresponds to a new hexapolar mode that does not exist in the circular 8 element SRR array. This is a consequence of the increased number of SRR elements as discussed above. The order of mode 4 at 1.65622 GHz is higher

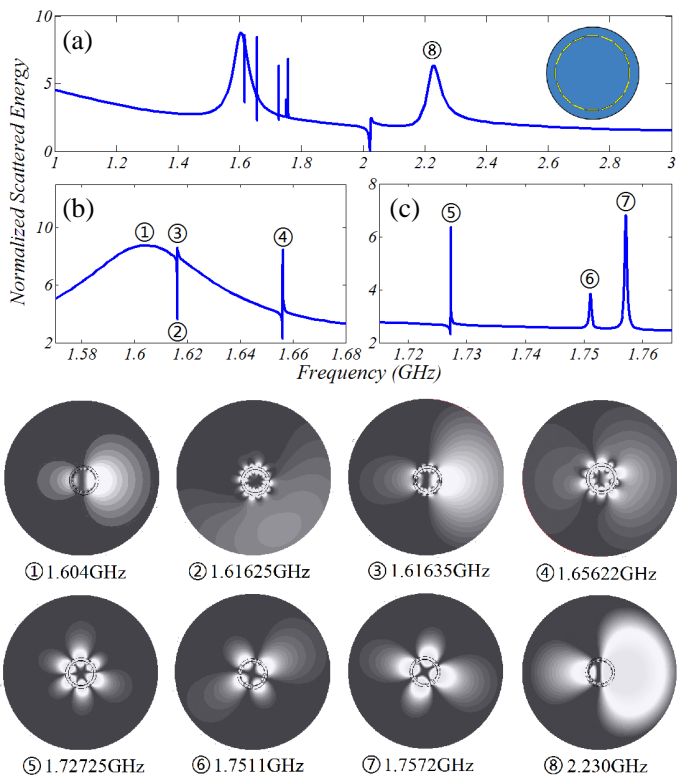


Figure 5. Blue curves: The normalized total energy scattered by the circular 16 element SRR array illuminated by a TE plane wave. The mode field patterns for peaks and dips of the spectrum labeled 1–8 are also plotted.

than the hexapolar mode 5, which is due to the fact that the lobe of mode 4 is smaller than that of mode 5, which in turn means a larger wave vector and thus a higher order mode. Mode 2 is another higher order mode with a much smaller lobe size as seen in the mode pattern. This is the highest order plasmonic like mode of the circular 16-element SRR array. The energy level of this highest order mode (having the narrowest bandwidth) is quite close to that of the dipolar mode (having the broadest bandwidth) and as a consequence the strong interaction between these two modes gives rise to an evident Fano line shape on the dipolar peak. This can clearly be seen from the field distributions changing from mode 1 to mode 3: the mode patterns of modes 1 and 3 are both dipolar like, and near the frequency of the narrow high order mode 2 the strong interaction of two different order modes

induces a deep dip of the scattering spectrum [27]. Mode number 8 is excited as the dielectric cylinder base is large enough to support a dipolar resonance at frequency 2.23 GHz. For the circular 16 element SRR array we also find the zero scattering position near the resonance frequency of the SRR at around 2.05 GHz (see the corresponding dip in the scattering spectrum).

5. CONCLUSION

To summarize, in this paper we have proposed circular SRR arrays and studied their scattering characteristics. By studying the scattering spectrum, we have found LSP like modes of the proposed structure, which scatters a much larger amount of energy of the incident wave than a dielectric or a PEC structure of same dimensions does. At the same time, at a certain frequency the proposed structure will not scatter any electromagnetic wave at all, acting as a zero scattering object.

We believe that the controllable scattering characteristics that the proposed structure displays may have important applications such as, e.g., a passive RFID tags which need large scattered field response to an incident wave or for cloaking applications as the structure is able to hide a dielectric target with high refractive index.

The use of SRR elements instead of a spoofed metal surface also expands SPP like wave behavior to TE polarization at low frequency bands.

ACKNOWLEDGMENT

The work is partially supported by the National Natural Science Foundation of China (No. 61108022), the National High Technology Research and Development Program of China (No. 2012AA030402), Guangdong Innovative Research Team Program (No. 201001D0104799318) the “111” Project, Swedish VR (No. 621-2011-4620) and AOARD.

REFERENCES

1. Pendry, J. B., A. J. Holden, W. J. Stewart, and I. Youngs, “Extremely low frequency plasmons in metallic mesostructures,” *Phys. Rev. Lett.*, Vol. 76, 4773–4776, 1996.
2. Pendry, J. B., A. J. Holden, D. J. Robbins, and W. J. Stewart, “Magnetism from conductors and enhanced nonlinear phenomena,” *IEEE Trans. Microwave Theory Tech.*, Vol. 47, 2075–2084, 1999.

3. Shelby, R. A., D. R. Smith, and S. Schultz, "Experimental verification of a negative index of refraction," *Science*, Vol. 292, 77–79, 2001.
4. Iwanaga, M., "First-principle analysis for electromagnetic eigen modes in an optical metamaterial slab," *Progress In Electromagnetics Research*, Vol. 132, 129–148, 2012.
5. Garcia, C. R., J. Correa, D. Espalin, J. H. Barton, R. C. Rumpf, R. Wicker, and V. Gonzalez, "3D printing of anisotropic metamaterials," *Progress In Electromagnetics Research Letters*, Vol. 34, 75–82, 2012.
6. Shalaev, V. M., "Optical negative-index metamaterials," *Nature Photonics*, Vol. 1, 41–48, 2007.
7. Schurig, D., J. J. Mock, B. J. Justice, S. A. Cummer, J. B. Pendry, A. F. Starr, and D. R. Smith, "Metamaterial electromagnetic cloak at microwave frequencies," *Science*, Vol. 314, 977–980, 2006.
8. Cai, W., U. K. Chettiar, A. V. Kildishev, and V. M. Shalaev, "Optical cloaking with metamaterials," *Nature Photonics*, Vol. 1, 224–227, 2007.
9. Cummer, S. A., B.-I. Popa, D. Schurig, D. R. Smith, and J. B. Pendry, "Full-wave simulations of electromagnetic cloaking structures," *Phys. Rev. E*, Vol. 74, 036621, 2006.
10. Danaeifar, M., M. Kamyab, A. Jafargholi, and M. Veysi, "Bandwidth enhancement of a class of cloaks incorporating metamaterials," *Progress In Electromagnetics Research Letters*, Vol. 28, 37–44, 2012.
11. Pendry, J. B., "Negative refraction makes a perfect lens," *Phys. Rev. Lett.*, Vol. 85, 3966–3969, 2000.
12. Zhang, Y., Y. Chuang, J. O. Schenk, and M. A. Fiddy, "Study of scattering patterns and subwavelength scale imaging based on finite-sized metamaterials," *Applied Physics A*, Vol. 107, 61–69, 2012.
13. Xie, Y., J. Jiang, and S. He, "Proposal of cylindrical rolled-up metamaterial lenses for magnetic resonance imaging application and preliminary experimental demonstration," *Progress In Electromagnetics Research*, Vol. 124, 151–162, 2012.
14. Hwang, R.-B., H.-W. Liu, and C.-Y. Chin, "A metamaterial-based *E*-plane horn antenna," *Progress In Electromagnetics Research*, Vol. 93, 275–289, 2009.
15. Ma, Y. G., C. K. Ong, T. Tyc, and U. Leonhardt, "An omnidirectional retroreflector based on the transmutation of dielectric singularities," *Nature Materials*, Vol. 8, 639–642, 2009.

16. Ma, H. F. and T. J. Cui, "Three-dimensional broadband and broad-angle transformation-optics lens," *Nature Communications*, Vol. 1, 124, 2010.
17. Talley, C. E., J. B. Jackson, C. Oubre, N. K. Grady, C. W. Hollars, S. M. Lane, T. R. Huser, P. Nordlander, and N. J. Halas, "Surface-enhanced Raman scattering from individual au nanoparticles and nanoparticle dimer substrates," *Nano Letters*, Vol. 5, 1569–1574, 2005.
18. Barnes, W. L., A. Dereux, and T. W. Ebbesen, "Surface plasmon subwavelength optics," *Nature*, Vol. 424, 824–830, 2003.
19. Maier, S. A., *Plasmonics: Fundamentals and Applications*, Springer, New York, 2007.
20. Zhang, Y., X. Zhang, T. Mei, and M. Fiddy, "Negative index modes in surface plasmon waveguides: A study of the relations between lossless and lossy cases," *Optics Express*, Vol. 18, 12213–12225, 2010.
21. Li, J., Y. Zhang, T. Mei, and M. Fiddy, "Surface plasmon laser based on metal cavity array with two different modes," *Optics Express*, Vol. 18, 23626–23632, 2010.
22. Tribelsky, M. I. and B. S. Luk'yanchuk, "Anomalous light scattering by small particles," *Phys. Rev. Lett.*, Vol. 97, 263902, 2006.
23. Pendry, J. B., L. Martín-Moreno, and F. J. Garcia-Vidal, "Mimicking surface plasmons with structured surfaces," *Science*, Vol. 305, No. 5685, 847–848, 2004.
24. Ma, Y. G., L. Lan, S. M. Zhong, and C. K. Ong, "Experimental demonstration of subwavelength domino plasmon devices for compact high-frequency circuit," *Optics Express*, Vol. 19, 21189–21198, 2011.
25. Ma, Y. G. and C. K. Ong, "Generation of surface-plasmon-polariton like resonance mode in microwave metallic gratings," *New Journal of Physics*, Vol. 10, 063017, 2008.
26. Pors, A., E. Moreno, L. Martín-Moreno, J. B. Pendry, and F. J. Garcia-Vidal, "Localized spoof plasmons arise while texturing closed surfaces," *Phys. Rev. Lett.*, Vol. 108, 223905, 2012.
27. Hao, F., T. Sonnefraud, P. V. Dorpe, S. A. Maier, N. J. Halas, and P. Nordlander, "Symmetry breaking in plasmonic nanocavities: Subradiant LSPR sensing and a tunable Fano resonance," *Nano Letters*, Vol. 8, 3983–3988, 2008.